

Prediction of Welding Deformation and Residual Stress of Stiffened Plates Based on Experiments

R X Bai, Z F Guo and Z K Lei *

State Key Laboratory of Structural Analysis for Industrial Equipment, Dalian University of Technology, Dalian 116024, China

*E-mail: leizk@163.com

Abstract. Thermo-elastic-plastic (TEP) method is a method that can accurately predict welding deformation and residual stresses, but the premise is to select the appropriate heat source parameters. Aiming at the two welded joints in the stiffened plate studied in this paper, the welding experiments of simple components were carried out respectively, and the corresponding welding deformation and residual stresses were measured. Based on the welding experiment, the corresponding TEP model was established, and the corresponding heat source parameters were obtained according to the experimental data. The comparison between the experimental results and the numerical results shows that the obtained heat source parameters can well predict the welding deformation and residual stress of the welded structure. And then, the obtained heat source parameters were applied to the TEP model of the stiffened plate. The prediction results show that the T-type fillet welds of the stiffened plate can reduce the angular deformation caused by the butt welds to a certain extent. In addition, we can also find that the heat of the subsequent welds can reduce the residual stresses at the completed welds. This method not only can save a lot of experimental costs and time, but also can accurately predict the welding deformation and residual stresses.

1. Introduction

The stiffened plate is often used in the structure of the ship to improve the carrying capacity of the panel and the whole structure. Welding is a commonly used metal connection process with high production efficiency and low production costs. However, the welding process also has unavoidable shortcomings [1] due to the high concentration of heat near the weld and rapid cooling of the cooling process, making the welding structure produce a certain welding deformation and residual stresses.

With the rapid development of computer performance and the wide application of finite element method, numerical simulation has become an effective and reliable method to predict the welding deformation and residual stress. Lee et al. [2] investigated the temperature field and residual stress of the dissimilar steel welding process. The simulation results show that the magnitude and distribution of the welding residual stresses of the dissimilar welds is different from the corresponding butt welds. Murakawa et al. [3] based on the inherent deformation method and applied the interface element to simulate the welding deformation of the thin plate structure. The numerical results agree well with the experimental results.

TEP method considering welding conditions and welding sequence in detail has been widely used in the prediction of welding deformation and residual stresses, which can more accurately predict the



welding deformation and residual stresses compared to other methods such as inherent strain method. T. Schenk [4] studied the effect of support distance on the welding deformation of T-joints. Wei[5] presents a validated TEP model to investigate the effect of the welding sequence on weld induced residual stress distributions in a multi-pass welded piping branch junction.

In this paper, we propose a method to obtain the appropriate heat source parameters based on the simple structure welding experiment and apply the parameters to the prediction of welding deformation and residual stresses of large and complex structures. Based on this method, T-beam welding and plate-butt welding are carried out for the two welds in the stiffened plate, and the corresponding welding deformation and residual stresses are measured. Based on the welding experiment, the corresponding TEP model was established to obtain the appropriate heat source parameters and then the parameters was applied to the welding analysis of the stiffened plate.

2. Welding experiment

2.1. T-beam welding experiment

For the fillet weld in the stiffened plate, the T-beam is welded with a wing size of 500x200x10mm and a web size of 500x380x6mm, as shown in figure 1. The welding method was manual arc welding (MAW) by a Panasonic YD-400SS3HGE welding machine and the welding conditions are given in Table 1. The material is 1045 steel, and the material composition and mechanical properties are shown in Table 2. The in-plane displacement of the web was measured using 2D-DIC, and the Y-displacement shift on a1 and a2 along Line2 was measured using a displacement meter with the precision of 0.05mm. The vernier caliper with precision of 0.01mm was used to obtain the Z-displacement on b1 and b2.

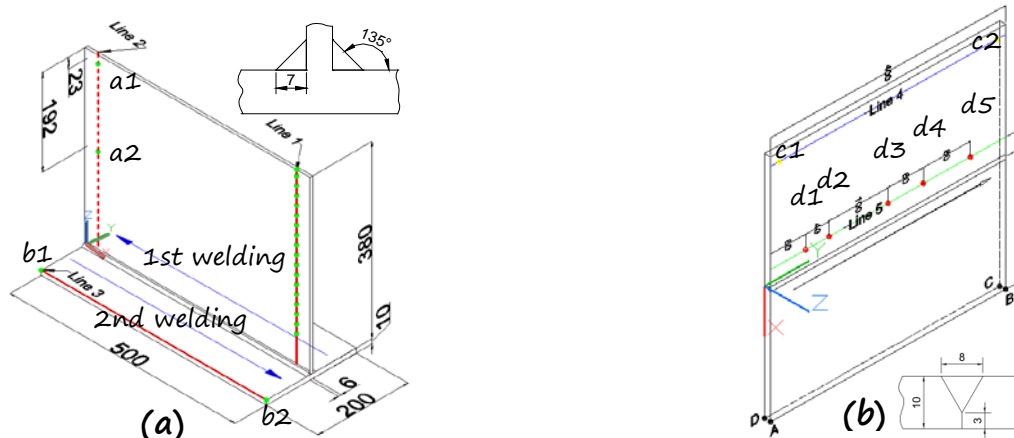


Figure 1. Geometric model and measuring points of (a) T-Beam (b) butt welding plate

Table 1. Welding conditions

Seam Type	Welding method	Wire	Pass number	Welding voltage (V)	Welding current (A)	Welding speed (mm/s)	Welding thermal efficiency
T-fillet welds	MAW	J507	1,2	64	130	4	0.6
Butt weld	MAW	J507	1	64	130	2.797	0.6

2.2. Plate butt welding experiment

In order to obtain the heat source parameters during butt welding, the plate butt welding experiment was carried on. Two 1045 steel plates with a length of 400 mm, a width of 200 mm and a thickness of 10 mm were used for butt welding, as shown in figure 1, the weld size was also shown. The Z-

displacement of c1 and c2 was measured by YHD-50 displacement meter with the precision of 0.05mm.

Table 2. 1045 steel material composition and mechanical properties

Chemical composition (%)						Mechanical properties	
C	Si	Mn	P	S	Cr	Yield Strength (MPa)	Tensile Strength (MPa)
0.46	0.24	0.59	0.016	0.005	0.01	366	642

According to GB / T 31310-2014 standard, the strain release coefficient $A = -4.587 \times 10^{-7} \text{ mm}^2/\text{N}$ and $B = -7.04 \times 10^{-7} \text{ mm}^2/\text{N}$ were obtained by calibration experiment. And the release strain ε_0 , ε_{45} and ε_{90} at d1-d5 were obtained by drilling method, as shown in figure 1. Thereby the transverse residual stresses and the longitudinal residual stresses can be obtained at d1-d5.

3. Validation of FEM model

3.1. Finite element simulation

The TEP analysis is a sequentially coupled finite element method that the nodal temperatures captured in the thermal analysis were applied as loads in the mechanical analysis. In the thermal analysis, two kinds of boundary conditions, convective heat transfer and radiant heat transfer are considered, and they are expressed by the composite heat release coefficient (CHRC), as shown in equation (1) and Table 3. In the mechanical analysis, the boundary condition is only to avoid the occurrence of rigid body displacement. Thermal analysis and mechanical analysis use the same element meshes, only the different types of element: Solid70 and Solid185 were used respectively. We assume that the material at the weld is the same as the base metal, and the changes in material properties with temperature were taken into account in the numerical simulations [6], as shown in figure 2.

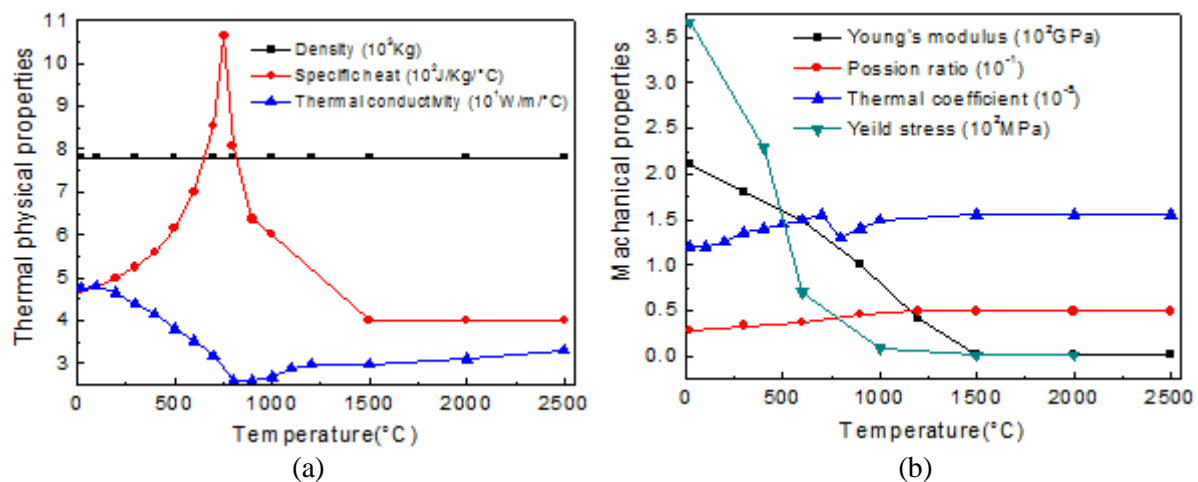


Figure 2. Temperature-dependent (a) thermal properties and (b) mechanical properties

$$q_h = \alpha_h (T - T_0) \quad (1)$$

Where q_h is heat loss due to convection and radiation, α_h is used to represent the composite heat dissipation coefficient.

Table 3. Temperature-dependent CHRC

Temperature (°C)	20	100	500	750	1000	1500	2000
CHRC ($\text{W} \cdot \text{m}^{-2}/^\circ\text{C}$)	1.336	6.68	33.4	91.15	148.9	264.4	379.9

For T-type fillet welds, the combined heat source model can more accurately describe the distribution of welding heat [7]. In this paper, a volumetric heat source and surface heat source with uniform density are used to express droplet heat and arc heat respectively, as shown in equation (2) and (3). And for the plate butt welds, the moving volumetric heat source is used.

$$Q_v = \frac{\beta \eta UI}{V} \quad (2)$$

Where U and I are the welding voltage and current, V is the heat source volume. η is the welding thermal efficiency. The coefficient β is the proportion coefficient between the homogeneous surface heat source and the total welding heat. Generally, $\beta = 0.6$ [8].

$$Q_A = \frac{(1 - \beta) \eta UI}{A} \quad (3)$$

Where A is the arc surface area.

The finite element model of T-beam and plate butt welding is shown in figure 3. In order to take into account the computational efficiency and accuracy, a dense mesh is used near the weld, and the element size increases as the distance from the weld increases. In the finite element model of T-beam, the length of each element in the welding direction is 10 mm, and the smallest element in the finite element models are 1 mm×1mm×10 mm. And in the finite element model of plate butt welding, the element size is the same as above, except for the length in the welding direction, which is 5 mm in length.

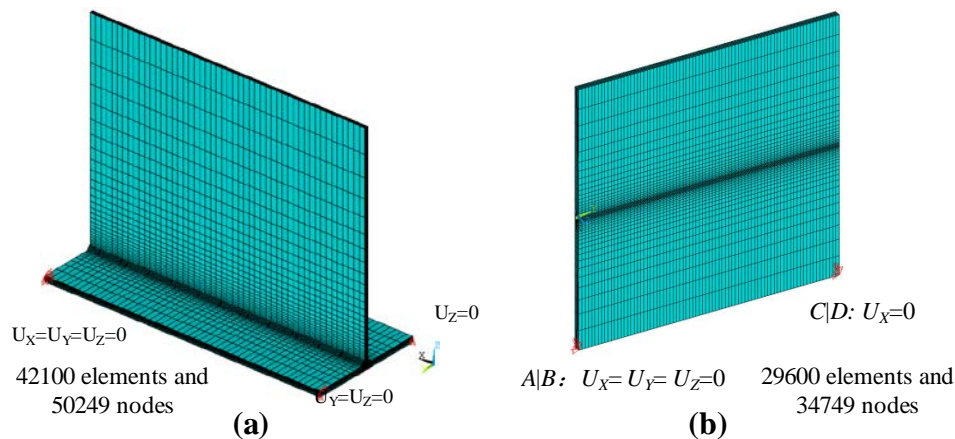


Figure 3. Finite element model of (a)T-Beam (b) butt welding plate

3.2. Comparison between experiment and numerical simulation

Figure 4 compares the welding deformation of T-beam welding experiments and numerical simulations. We can see that the numerical simulation results are in good agreement with the experimental results, not only accurately reflect the welding deformation trend, but also accurately predict the welding deformation value.

Figure 5 shows the results of the plate butt welding experiments and the numerical simulation of the welding deformation and residual stresses. For the most important welding deformation, ie, the angular deformation, the experimental results agree well with the numerical results. For the residual stresses, the minimum error is the transverse residual stress at the Y coordinate of 0.34 m, which is 1.13 MPa. And the maximum error is the longitudinal residual stress at the Y coordinate of 0.26 m, which is 156.82 MPa. The reason is that, in the actual welding process, the two flat plates are welded together with the formation of the weld pool, while in the finite element simulation, prior to the start of welding, the two plates are bonded together, causing the error of finite element results with the

experimental results, and this effect is more pronounced in the longitudinal direction. So the numerical results of the transverse residual stresses agree well with experimental results. In general, the numerical simulation results accurately describe its trend, and the error between the two is very weak except for the individual measurement points.

From the above analysis we can see that the finite element model and the selected heat source parameters can accurately predict the welding deformation and residual stresses.

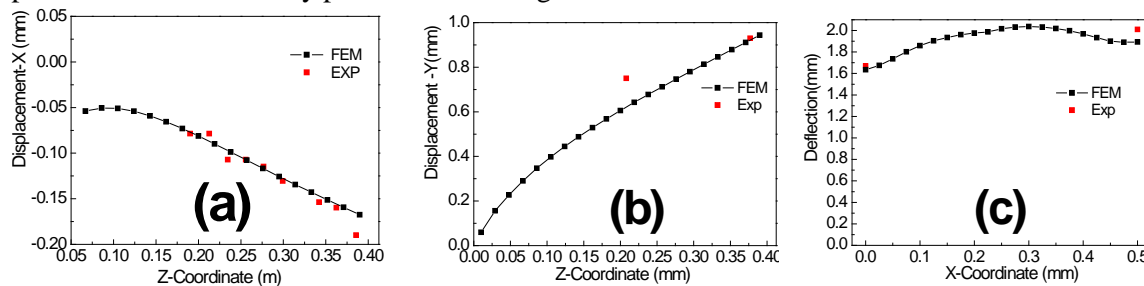


Figure 4. Comparison of T-beam welding experiment and numerical simulation: (a) X-displacement along Line 1 (b) Y-displacement along Line 2 (c) Z-displacement along Line 3

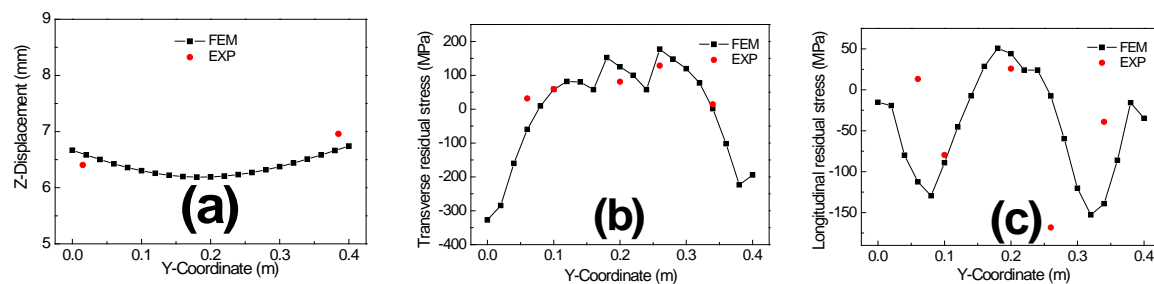


Figure 5. Comparison of plate butt welding experiment and numerical simulation: (a) Z-displacement along Line 4, (b) Transverse residual stresses along Line 5, (c) Longitudinal residual stresses along Line 5.

4. Prediction of welding deformation and residual stress of stiffened plates

The heat source parameters obtained above were applied to thermal analysis to simulate the temperature field. And then, the temperatures obtained in the thermal analysis were applied as a load in the mechanical analysis to solve the welding deformation and residual stresses.

Figure 6 shows the geometric model and dimensions of the stiffened plate. The dimensions of the two welds are shown in figure 1. Using the same geometric size and element size of the finite element model of plate butt welding, the finite element model was established, as shown in figure 7, with a total of 86880 elements, 97767 nodes. And the welding sequence is also shown in figure 6, that is, the butt weld is first welded, then the left fillet weld, and finally the right fillet weld.

Figure 8 shows the total displacement of the stiffened plate. We can see that the main deformation mode is transverse bending, and the displacement at the left bar is the largest, while the longitudinal bending is almost negligible. This is due to the large thickness of the stiffened plate. At the same time, we can find that the deformation at the end of the weld is larger than the beginning of the weld. The reason is that the base metal is more resistant to the welding deformation due to the low temperature of the structure at the beginning of the welding, while the base metal is less resistant to the welding deformation due to the higher temperature of the structure at the end of the welding.

Figure 9 demonstrates the Y-direction displacement along Line 6, and the curve is symmetrical about the butt weld. We can see that in the vicinity of the butt weld, the trend of increasing deformation is gradually reduced, and the deformation is reduced near the butt weld, which is caused by the angular deformation of the T-type fillet welds on both sides.

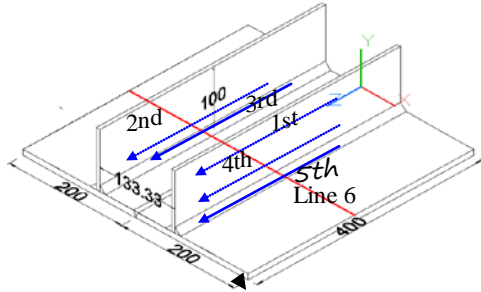
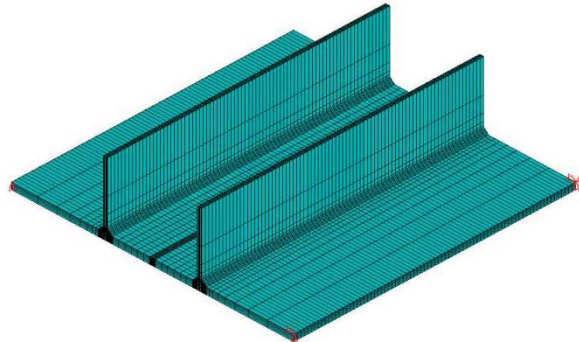
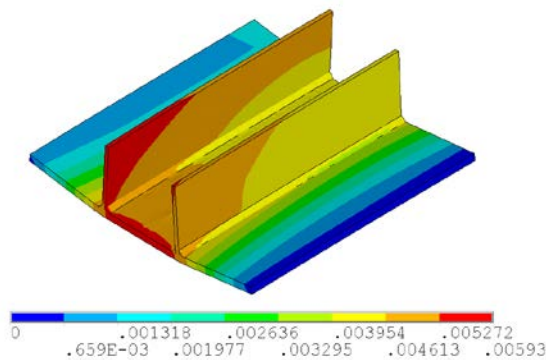
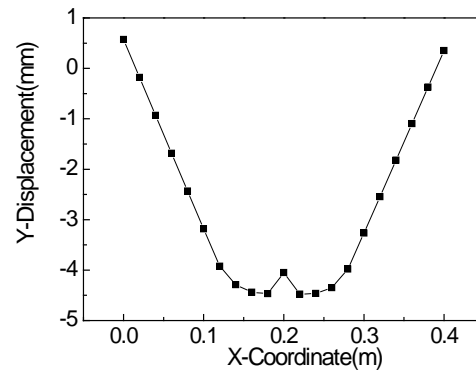
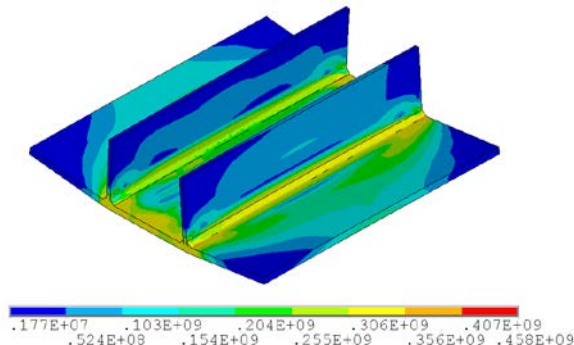
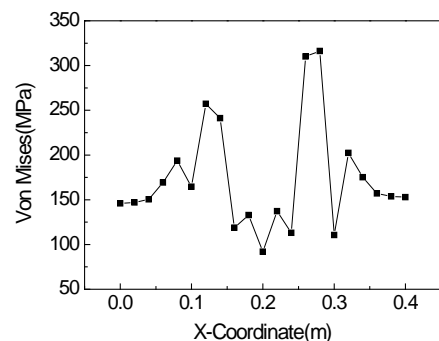
**Figure 6.** Geometrical model of stiffened plate**Figure 7.** Finite element model of stiffened plate**Figure 8.** Total displacement of the stiffened plate**Figure 9.** Y-Displacement along Line 6

Figure 10 shows the equivalent von Mises stress of the stiffened plate with greater stresses at the weld and less stresses away from the weld zone, and the largest residual stress occurred in the weld start / end. Figure 11 shows the magnitude and distribution of the Mises stress along Line 6. We can see that the maximum stress is close to the yield stress of the 1045 steel, which has a negative effect on the service performance of the stiffened plate. Through the careful observation we can find that the residual stresses at the butt weld is less than that of the left T-type fillet, while the left T-shaped fillet is less than the right. This is due to the fact that the completed welds surf from thermal effect from the lateral welds, so that the residual stresses is released.

**Figure 10.** Mises stress distribution of the stiffened plate**Figure 11.** Mises stress along Line 6

5. Conclusion

In this paper, the corresponding TEP model is established according to the simple welding experiments, and the appropriate heat source parameters are obtained. The numerical results agree well

with the experimental results. Applying of the heat source parameters, the welding deformation and residual stresses of the stiffened plates are predicted, and the following conclusions were drawn.

- (1) This paper presents a method to obtain accurate heat source parameters based on simple welding structures and to apply them to the prediction of welding deformation and residual stresses of large welded structures.
- (2) The T-type fillet welds of the stiffened plate reduce the angular deformation caused by the butt welds to a certain extent.
- (3) The equivalent Mises stress at the welds is very large and close to the yield stress.
- (4) The heat of the subsequent welds has a thermal effect on the completed welds, which can reduce the residual stresses at the completed welds.

Acknowledgement

This research was financially supported by the National Natural Science Foundation of China (Nos. 11472070, 11772081, 11572070), the Natural Science Foundation of Liaoning Province of China (No.2015020145).

References

- [1] Lee C H and Chang K H, 2012, *Appl Therm Eng.*, Temperature fields and residual stress distributions in dissimilar steel butt welds between carbon and stainless steels, Vol **45-46**, pp. 33-41.
- [2] Deng D, 2009, *Mater Des.*, FEM prediction of welding residual stress and distortion in carbon steel considering phase transformation effects, Vol **30**, pp. 359-66.
- [3] Murakawa H, Deng D A, Ma N S and Wang J C, 2011, *Comput. Mater. Sci.*, Applications of inherent strain and interface element to simulation of welding deformation in thin plate structures, Vol **51**, pp. 43-52.
- [4] Schenk T, Doig M, Esser G and Richardson I M, 2010, *Sci. Technol. Weld. Join.*, Influence of clamping support distance on distortion of welded T joints, Vol **15**:7, pp. 575-82.
- [5] Wei J and Yahiaoui K, 2012, *Int J Press Vessels Piping.*, Effect of welding sequence on residual stress distribution in a multipass welded piping branch junction, Vol **95**, pp. 39-47.
- [6] Gao K, Qin X P, Wang Z, Chen H, Zhu S X, Liu Y X and Song Y L, 2014, *J. Mater. Process. Technol.*, Numerical and experimental analysis of 3D spot induction hardening of AISI 1045 steel, Vol **214**, pp. 2425-33.
- [7] Deng D A, Liang W and Murakawa H, 2007, *J. Mater. Process. Technol.*, Determination of welding deformation in fillet-welded joint by means of numerical simulation and comparison with experimental measurements, Vol **183**, pp. 219-25.
- [8] Pardo E and Weckman D C, 1989, *Metall. Trans. B*, Prediction of weld pool and reinforcement dimensions of GMA welds using a finite element model, Vol **20B**, pp. 937-47.